

CERN-TH/97-321

Non-Perturbatively Improved Quenched Hadron Spectroscopy

A. Cucchieri^a, M. Masetti^a, T. Mendes^a, R. Petronzio^{a,b}

^a*Dipartimento di Fisica, Università di Roma “Tor Vergata”
and INFN, Sezione di Roma II*

Via della Ricerca Scientifica 1, 00133 Rome, Italy

^b*CERN, Theory Division, CH-1211 Geneva 23, Switzerland*

Abstract

We make a quenched lattice simulation of hadron spectroscopy at $\beta = 6.2$ with the Wilson action non-perturbatively improved. With respect to the unimproved case, the estimate of the lattice spacing is less influenced by the choice of input hadron masses. We study also the effects of using an improved quark mass in the fits to the dependence of hadron masses upon quark masses.

CERN-TH/97-321
November 1997

1 Introduction

The computational cost of the extrapolation to the continuum limit of lattice QCD simulations can be significantly reduced by using improved actions, where the leading cutoff effects are cancelled by suitable counterterms. It has been shown that $O(a)$ on shell improvement is achieved by adding to the usual Wilson action the clover term, with a coefficient that has been recently determined non-perturbatively by the ALPHA collaboration [2, 3].

We present here the results of our study of hadron spectroscopy using the non-perturbatively clover-improved Wilson action

$$S = S_W + c_{SW} a^5 \frac{i}{4} \sum_x \bar{\Psi}(x) \sigma_{\mu\nu} \hat{F}_{\mu\nu} \Psi(x), \quad (1)$$

where S_W is the standard Wilson action and the second term is the naive continuum limit of the clover term (see [2] for details). Preliminary results have been reported in [1].

We consider a lattice volume of $24^3 \times 48$ and a coupling $\beta = 6.2$. According to [2, 3], we thus take $c_{SW} = 1.61375065$. We choose the following values for the hopping parameter κ : 0.1240, 0.1275, 0.1310, 0.1340, 0.1345, 0.1350, 0.1352. The simulations were carried out on the 512 processor computer of the APE100 series at Tor Vergata.

Our statistics come from 104 quenched gauge configurations, generated by a hybrid over-relaxation algorithm, with each update corresponding to a heat-bath sweep followed by three over-relaxation sweeps. The configurations are separated by 1000 updates.

The inversion of the fermion matrix is performed using the stabilized biconjugate gradient algorithm [4]. We restart the inversion from the current solution every 100 iterations, in order to reduce the accumulation of roundoff errors [5]. We employ point-like sources. We sum fermion propagators over the space directions x, y, z for sites within blocks of side 3, and then store the result. We then form hadron correlations from these “packed” propagators. This procedure differs from the exact computation of hadron correlations by gauge-non-invariant terms and becomes exact in the limit of an infinite number of configurations (in our case we have checked that the errors thus introduced are negligible). This corresponds to gaining a factor 3^3 in storage, and has enabled us to have all quark propagators stored simultaneously. In this way we can form “off-line” hadron correlations from non-degenerate combinations of quark flavours.

Hadron masses are obtained from single mass fits to the large time behaviour of zero momentum hadron correlators. A two mass fit has also been done, but the results for the higher mass were too unstable to quote numbers. The value for the lower mass turned out to be totally compatible with the single mass fit. The errors are estimated through a jack-knife procedure. In order to improve the stability in time of the plateau where a single hadron dominates the correlation for the baryons, in some

cases we have averaged the correlation over a fixed number of lattice spacings in the time direction: the resulting correlation maintains its exponential behaviour with a coefficient depending upon the size of the smearing. This procedure turned out to be very useful for the determination of baryon mass splittings where we also made fits directly to the ratio of correlations to minimize the effects of collective fluctuations. We report in Table 1 our results for hadron masses in lattice units and at the various values of κ .

κ	M_{PS}	M_V	M_N
0.1240	1.0737(20)	1.0997(15)	1.7002(35)
0.1275	0.8532(20)	0.8873(15)	1.3774(35)
0.1310	0.6048(20)	0.6565(20)	1.0189(40)
0.1340	0.3445(20)	0.4364(35)	0.6608(65)
0.1345	0.2909(25)	0.3977(50)	0.5937(85)
0.1350	0.2294(30)	0.364(10)	0.520(15)
0.1352	0.2007(40)	0.353(15)	0.483(20)

Table 1: Masses in lattice units (diagonal-flavour combinations only) for the pseudoscalar and vector mesons, and for the nucleon.

2 Lattice Spacing and Meson Masses

In order to extract physical values from lattice data, one needs to interpolate the results at appropriate values of quark masses, and to give them physical values by a suitable normalization. These steps imply a number of choices.

The first concerns the determination of “ κ_c ”: indeed, the renormalization of the quark mass with Wilson fermions is not multiplicative, and the critical value of the hopping parameter is shifted from its free-case limit. Within the improvement programme one can determine the critical value κ_c using the mass extracted from an improved Ward identity, defined as [2]

$$m_{WI} \equiv \frac{\langle \partial_\mu \{A_\mu^{(bare)} + c_A a \partial_\mu P^{(bare)}\} \mathcal{O} \rangle}{2 \langle P^{(bare)} \mathcal{O} \rangle} .$$

with the parameter c_A fixed from ref. [2] to -0.037 . A linear extrapolation to the limit of $m_{WI} = 0$, using the first five points obtained from the combinations of the three highest κ values, provides a fit for the determination of κ_c much more stable than the conventional fit of pseudoscalar meson masses to the limit of zero pion mass. Our results for κ_c are:

$$\text{from } m_{WI} = 0 \quad \kappa_c = 0.135828(5)$$

$$\text{from } M_{PS}^2 = 0 \quad \kappa_c = 0.135849(13).$$

The values of the parameters of a linear fit in $1/\kappa$ to M_{PS}^2 and to m_{WI} are:

$$m_{WI} = -3.8059(15) + 0.5169(2) \times (1/\kappa) \quad (2)$$

$$M_{PS}^2 = -8.38(3) + 1.138(4) \times (1/\kappa). \quad (3)$$

The residual discrepancy between the two values of κ_c is a signal of residual lattice artefacts.

Once the choice for the value for κ_c from m_{WI} has been made, we make a second choice that improves the fits to the dependence of hadron masses upon quark masses: instead of using the bare quark mass, defined as $m_q(\kappa) \equiv (1/\kappa - 1/\kappa_c)/2$, we use an “improved” bare quark mass [2] defined by

$$\tilde{m}_q(\kappa) \equiv m_q(\kappa) [1 + b_m m_q(\kappa)]. \quad (4)$$

(Note that \tilde{m}_q is the renormalized mass with $Z_m = 1$.) The improvement coefficient b_m has been determined non-perturbatively [7]: $b_m = -0.62(3)$.

For non-degenerate flavour cases we use symmetric averages of the masses defined above, e.g. for a meson corresponding to the flavours κ_1 and κ_2 , we define $\tilde{m}_q(\kappa_1, \kappa_2) \equiv [\tilde{m}_q(\kappa_1) + \tilde{m}_q(\kappa_2)]/2$. Similarly, for baryons, we define m_q and \tilde{m}_q as the symmetric average of the quark masses for the three flavours. Note that when using averages of the improved masses we reabsorb in the mass definition terms that are quadratic in the quark masses. This may and does change the estimates of the deviation of hadron masses (their squares for pseudoscalars) from a linear dependence upon the quark masses. For baryons the choice of the improved mass does extend the linear behavior substantially beyond the light-mass region.

A third choice to be made is on the physical inputs that give physical units to the lattice spacing and to the lattice masses.

The lightest of our quark masses is in the strange quark mass region and we decided to use physical inputs at the strange quark mass for the lattice spacing to avoid the inclusion of systematic uncertainties deriving from a chiral extrapolation. A known deficiency of the quenched approximation is the estimate of vector-pseudoscalar mass splittings. In particular the experimental difference of the squares of vector and pseudoscalar masses is essentially constant as a function of the quark mass, a feature that is not reproduced by present quenched data. Besides possible unquenching effects, this can be ascribed to lattice artefacts, which should be partially cancelled in our simulation.

For the strange mesons, we decided to use as input just such a square-mass difference: this can be seen as an attempt to reabsorb the residual lattice artefacts in a redefinition of the quark mass. More in detail, we first fix the value of the strange quark mass from the ratio:

$$(M_V^2 - M_{PS}^2)/M_V^2 \quad (5)$$

using the experimental value for K and K^* meson masses as input, and then we extract the lattice spacing by normalizing the K^* mass to its experimental value. This gives the following values:

$$m_s = 0.0315(45) \quad \text{and} \quad a^{-1} = 2561(100) \text{ MeV}, \quad (6)$$

where we have used, for the average values, quadratic and linear mass fits, respectively. These are the values of m_s and a^{-1} adopted in this paper. In the following we will not include the overall error coming from the uncertainty of the lattice spacing when quoting errors for hadron masses in physical units. This amounts to an overall and systematic uncertainty of about 4%.

Our fits for M_V and M_{PS}^2 in the light/strange quark mass region are given below.

- **Linear** fits in terms of the **improved** quark mass:

$$M_V = 0.309(20) + 2.49(55) \times \tilde{m}_q \quad (7)$$

$$M_{PS}^2 = -0.001(2) + 2.398(35) \times \tilde{m}_q \quad (8)$$

- **Quadratic** fits in terms of the **improved** quark mass:

$$M_V = 0.298(15) + 2.82(50) \times \tilde{m}_q + 1.0(35) \times \tilde{m}_q^2 \quad (9)$$

$$M_{PS}^2 = 0.005(2) + 1.992(50) \times \tilde{m}_q + 7.53(40) \times \tilde{m}_q^2 \quad (10)$$

- **Linear** fits in terms of the **unimproved** quark mass:

$$M_V = 0.311(20) + 2.38(55) \times m_q \quad (11)$$

$$M_{PS}^2 = 0.000(2) + 2.328(30) \times m_q \quad (12)$$

- **Quadratic** fits in terms of the **unimproved** quark mass:

$$M_V = 0.304(15) + 2.60(45) \times m_q + 0.4(30) \times m_q^2 \quad (13)$$

$$M_{PS}^2 = 0.004(2) + 2.085(50) \times m_q + 3.91(35) \times m_q^2 \quad (14)$$

The quadratic fit for the pseudoscalar meson gives evidence for a quadratic term, while for the vector case its presence appears very marginal. The coefficient of the quadratic term in the unimproved mass case is expected to be smaller than in the improved case from the relation in eq. (4).

The chiral limit of vector masses is obtained by linear extrapolation in terms of the improved quark mass, showing good agreement when compared to the experimental value. This indicates that a lattice spacing extracted from the chiral limit leads to a value very close to the one in eq. (6):

$$a_{chiral}^{-1} = 2486(175) \text{ MeV}. \quad (15)$$

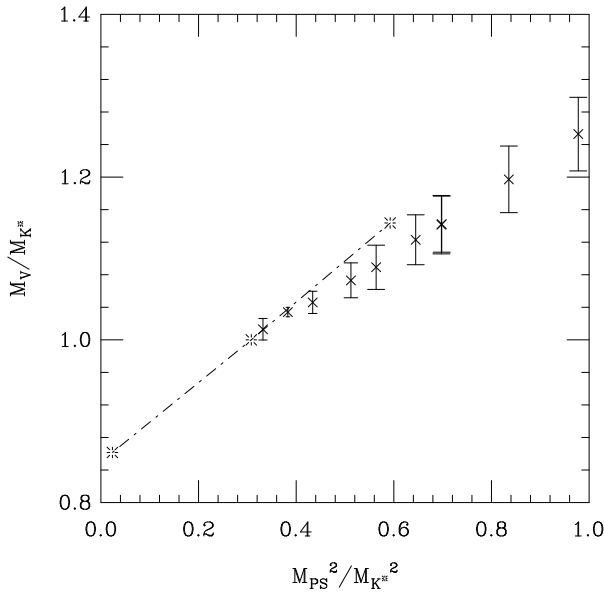


Figure 1: APE plot for M_V .

The fit for the vector case goes through the ϕ mass with reasonable accuracy and indicates that in the strange quark mass region a lattice spacing normalization from the ϕ would also give similar results:

$$a_\phi^{-1} = 2634(40) \text{ MeV.} \quad (16)$$

In Fig. 1 we show a plot of the vector meson mass as a function of M_{PS}^2 . The masses are normalized to the K^* meson mass, taken at the strange quark mass value given in the eq. (6) above. The asterisks correspond to the physical values for the ratio.

As can be seen from this figure, the experimental slope dM_V/dM_{PS}^2 is different from the one corresponding to our data. This is related to the behaviour of the quantity J defined by:

$$J \equiv M_V (dM_V/dM_{PS}^2), \quad (17)$$

obtained from M_V as a function of M_{PS}^2 . Our results for J are quoted in Table 2. They are rather similar to those obtained without improvement (for a recent review, see [8]), although slightly closer to the experimental result.

The procedure used to determine the strange quark mass fails when applied to the charm case: it is not possible here to find a value of the quark mass that reproduces the observed splitting. Therefore, we decided to define the charm quark mass from a

	Exp. value	Our value
J_{K^*}	0.487	0.40(11)
J_ϕ	0.557	0.45(12)

Table 2: Values of the quantity J and comparison with experiment.

fit to the ratio $M_{PS}^2/M_{K^*}^2$. We get

$$m_c = 0.388(25) \text{ from } m_q, \quad (18)$$

$$m_c = 0.3154(10) \text{ from } \tilde{m}_q. \quad (19)$$

By using the “ K^* ” lattice spacing we obtain for the D^* charmed meson:

$$M_{D^*} = 1955(6) \text{ MeV (exp. value 2008 MeV).} \quad (20)$$

The above value for the vector mass comes from a linear fit to a cluster of points around the improved charm quark mass.

For the vector meson with an unimproved quark mass we find:

$$M_{D^*} = 1981(5) \text{ MeV.} \quad (21)$$

In both cases, the underestimate of the experimental pseudoscalar-vector mass splitting is not dramatic.

The value of the lattice-improved strange quark mass given in eq. (6) can be used to obtain the strange quark mass in physical units. Firstly, we multiply it by the mass renormalization factor Z_m at the $(1/a)$ scale, using the tadpole-improved formula given in eq. (41) of ref. [9]. We then evolve the result to the 2 GeV scale with a perturbative renormalization group factor as in [10]. We get

$$m_s = 111(15) \text{ MeV.} \quad (22)$$

This result is in agreement with that of ref. [9].

In the ratio of charm over strange quark mass the renormalization factor Z_m drops out and we can give a value for the ratio of renormalized quark masses:

$$\begin{aligned} m_c/m_s &= 12.1 \pm 1.6 \text{ from } m_q, \\ m_c/m_s &= 10.0 \pm 1.4 \text{ from } \tilde{m}_q. \end{aligned}$$

Notice that the difference comes essentially from the reduction of the charm quark mass going from the unimproved to the improved bare quark mass definition (see eq. (19)).

We can use this ratio, combined with the theoretical prediction of 1.220(60) GeV for the charm quark mass [11], to obtain an independent evaluation of the strange

quark mass. After evolving this value of the charm quark mass to the 2 GeV scale, we get:

$$\begin{aligned} m_s &= 92(13) \text{ MeV from } m_q, \\ m_s &= 111(16) \text{ MeV from } \tilde{m}_q. \end{aligned}$$

The value obtained using the improved bare quark mass is in very good agreement with the determination in eq. (22).

3 Baryon Masses

In this section we report our results for baryon masses and baryon mass splittings. We show APE plots for the octet and for the decuplet baryons in Fig. 2. Note that we divide at each point by M_V , interpolated to the strange-quark mass, corresponding to M_{K^*} (i.e. a constant value). Experimental points in these figures (asterisks) correspond to M_N , M_Σ and M_Ξ and appropriate meson masses in Fig. 2a, and similarly M_Δ , M_{Σ^*} , M_{Ξ^*} and M_Ω for Fig. 2b.

We have considered non-relativistic wave functions. The correlators for the spin-3/2 (decuplet) baryons are completely symmetric in flavour. We therefore expect to observe a smooth behaviour of their masses in terms of the average quark masses m_q and \tilde{m}_q . For the spin-1/2 (octet) baryons, on the contrary, the correlators are not completely flavour-symmetric. We have two types of correlators (see [6] for details): Σ -like (e.g. for the proton, neutron, Σ and Ξ) and Λ -like (e.g. for Λ). The expressions for their masses from quenched chiral perturbation theory, in the case of two light quarks m_u and a strange quark m_s , are given by [6]:

$$M_\Sigma = M_0 + 4F m_u + 2(F - D) m_s \quad (23)$$

$$M_\Lambda = M_0 + 4(F - 2D/3) m_u + 2(F + D/3) m_s. \quad (24)$$

The constant D can be related to the Σ - Λ octet hyperfine splitting, as can be seen from the above formulae. We have considered fits as functions of the symmetric average masses described above also in the spin-1/2 case.

Note that we have defined the quantity

$$M_{oct} \equiv (M_N + M_\Lambda)/2, \quad (25)$$

which we construct from the appropriate ratios of correlators. This combination was chosen so that the resulting mass is flavour-symmetric. For this “octet” particle the advantage of using the improved quark mass is clearest, see Fig. 3.

From fits of the Σ - Λ mass splitting, and of M_{oct} , it is possible to extract the value of the constants D and F . We obtain:

$$D = -0.51(20) \quad (26)$$

$$F = 0.80(20). \quad (27)$$

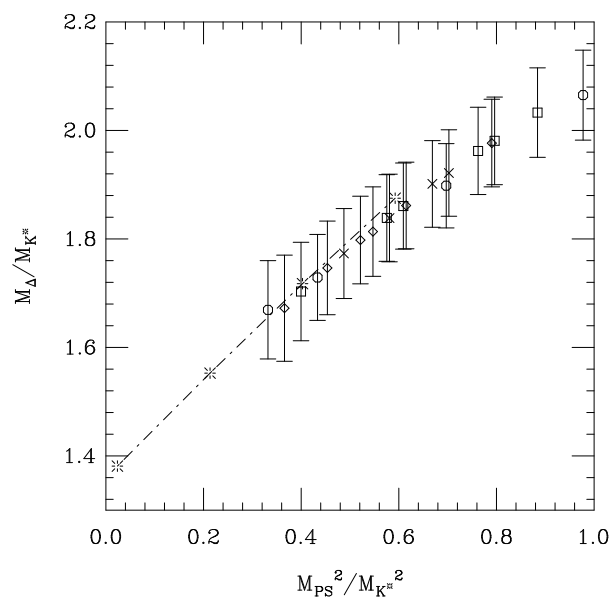
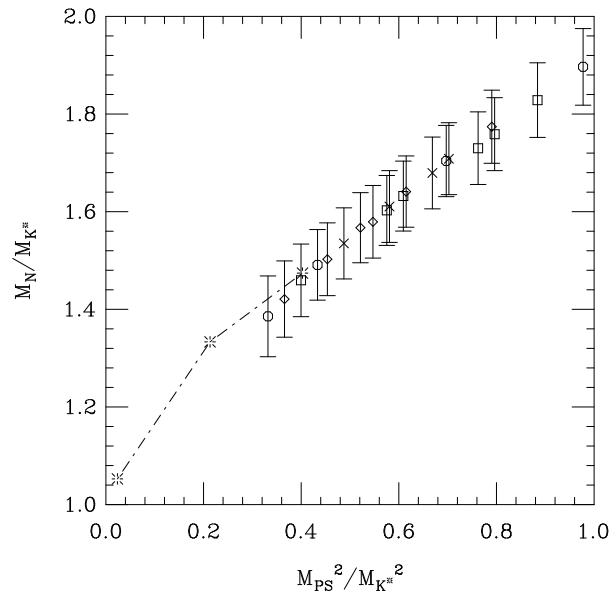


Figure 2: APE plot for (a) the nucleon mass (octet baryons) and (b) the Δ mass (decuplet baryons).

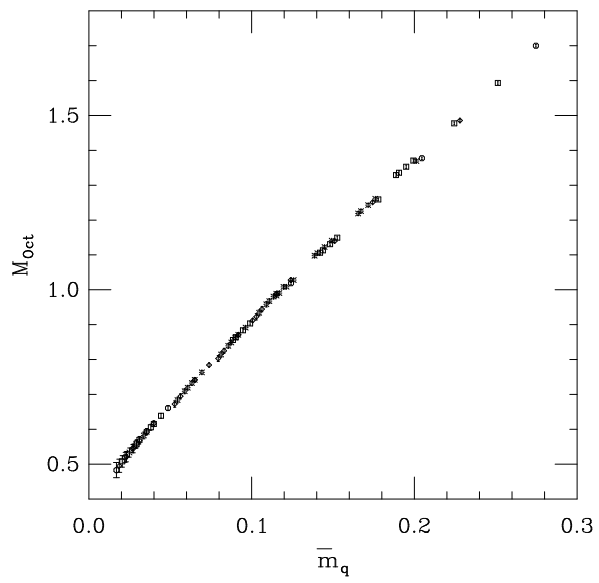
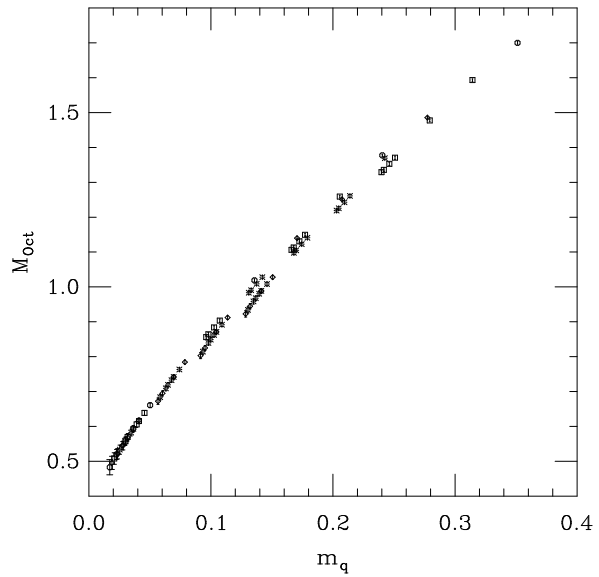


Figure 3: “Octet” mass in terms of (a) m_q (b) \widetilde{m}_q .

In Table 3 we give our baryon mass values in MeV. We have used in all cases linear fits of the masses as functions of the average improved bare quark mass \widetilde{m}_q , except for the $\Sigma-\Lambda$ mass splitting, where we used a quadratic fit. We have also included the predictions for charmed baryons using the improved quark mass.

	Exp. value	Our value
M_N	939	952(110)
M_Σ	1189.4	1148(60)
$M_{\Sigma-\Lambda}$	73.7	70(30)
M_Δ	1232	1265(110)
$M_{\Delta-N}$	293	297(80)
M_{Σ_c}	2453	2406(15)
$M_{\Sigma_c-\Lambda_c}$	168	232(40)

Table 3: Baryon masses in MeV and comparison with experiment. The error in parentheses represents the statistical error, while the error due to the determination of the inverse lattice spacing is of about 4%.

4 Conclusions

The main effect of the non-perturbative improvement observed on hadron masses is a smaller spread in the value of the lattice spacing extracted from light mesons with and without strange quarks. We have also shown how the use of the improved quark mass turns the rough behaviour of the dependence of the octet baryon mass upon quark masses into a smooth one. We have found a remarkable agreement in the improved theory between two independent determinations of the strange quark mass, one normalized through the lattice spacing and the other from the value for the charm mass extracted in the continuum from charmonium spectrum calculations.

For an accurate comparison of these results with the unimproved case, we are presently analysing [12] on the same set of gauge configurations the case $c_{sw} = 0$.

References

- [1] T. Mendes, to appear in the proceedings of *Lattice '97*, hep-lat/9711023.
- [2] M. Lüscher et al., Nucl. Phys. **B478**, 365 (1996).
- [3] M. Lüscher et al., Nucl. Phys. **B491**, 323 (1997).
- [4] A. Frommer et al., Int. J. Mod. Phys. **C5**, 1073 (1994).

- [5] G. Cella et al., Int. J. Mod. Phys. **C7**, 787 (1996).
- [6] T. Bhattacharya et al., Phys. Rev. **D53**, 6486 (1996).
- [7] G.M. de Divitiis and R. Petronzio, [hep-lat/97100771](#).
- [8] T. Yoshié, [hep-lat/9711017](#).
- [9] M. Göckeler et al., [hep-lat/9707021](#).
- [10] R. Gupta and T. Bhattacharya, Phys. Rev. **D55**, 7203 (1997).
- [11] *Review of Particle Physics*, Particle Data Group, Phys. Rev. **D54**, 308 (1996).
- [12] A. Cucchieri et al., *Comparison of improved and unimproved quenched hadron spectroscopy*, in preparation.